

KOSZALIN UNIVERSITY OF TECHNOLOGY

**RESEARCH AND MODELLING
IN CIVIL ENGINEERING
2018**

Edited by
Jacek Katzer, Krzysztof Cichocki and Jacek Domski

KOSZALIN 2018

MONOGRAPH NO 355
FACULTY OF CIVIL ENGINEERING,
ENVIRONMENTAL AND GEODETIC SCIENCES

ISSN 0239-7129
ISBN 978-83-7365-502-7

Chairman of the University Editorial Board
Zbigniew Danielewicz

Editors
Jacek Katzer, Krzysztof Cichocki and Jacek Domski
Koszalin University of Technology, Poland

Reviewers
Jacek Gołaszewski – Silesian University of Technology, Poland
Wojciech Sumelka – Poznań University of Technology, Poland

Technical editor
Czesław Suchocki

Website editor
Mariusz Ruchwa

Linguistic consultations
Ewa Sokółowska-Katzer

Typesetting
Czesław Suchocki

Cover design
Tadeusz Walczak

www.cecem.eu

© Copyright by Koszalin University of Technology Publishing House
Koszalin 2018

KOSZALIN UNIVERSITY OF TECHNOLOGY PUBLISHING HOUSE
75-620 Koszalin, Raławicka 15-17, Poland

Koszalin 2018, 1st edition, publisher's sheet 13,42, circulation 120 copies
Printing: INTRO-DRUK, Koszalin, Poland

Table of contents

1. Relationship between mechanical properties and conductivity of SCC mixtures with steel fibres	7
2. Quantitative comparison between visual and UAV-based inspections for the assessment of the technical condition of building facades	19
3. Choice of optimal material solutions for the assessment of heat and humidity states of outer walls made using the technology of light steel framing	31
4. Behaviour of high performance concrete in mixed mode loadings: experiments and numerical simulation	45
5. Performance and optimization of prestressed beam with respect to shape dimensions.....	63
6. Plate strip in a stabilized temperature field and creep effect	87
7. Harnessing digital image correlation system for assessing flexural characteristics of SFRC based on waste ceramic aggregate.....	113
8. An experimental analysis of the determination of the elastic modulus of cementitious materials.....	129
9. X-ray investigation of steel fibres in high performance self-compacting concrete beams	149
10. Binary alkali-activated materials with brick powder.....	171
11. Numerical analysis of the temperature distribution in an office room	187
12. Generalized maximum tangential stress criterion in double cantilever beam specimens: choice of the proper critical distance	199
13. Comparison of pulse-echo-methods for testing of heat degradation concrete	213
14. Fundamental formulae for the calculation of shear flexible rod structures and some applications	237

5. Performance and optimization of prestressed beam with respect to shape dimensions

Tuan Duc Le¹, Pavlína Matečková² and Petr Konečný³

¹ Faculty of Civil Engineering, Saigon Technology University, 180 Cao Lo Str., Ward 4, Dist. 8, HCMC 70000, Vietnam, orcid.org/0000-0003-3188-6759

² Faculty of Civil Engineering, VSB – Technical University of Ostrava, Department of Structural Mechanics, L. Podeste 1875, 708 33 Ostrava-Poruba, Czech Republic, orcid.org/0000-0002-8049-3153

³ Faculty of Civil Engineering, VSB – Technical University of Ostrava, Department of Structural Mechanics, L. Podeste 1875, 708 33 Ostrava-Poruba, Czech Republic, orcid.org/0000-0001-6667-7522

Abstract: The chapter deals with the performance and optimization of prestressed concrete beam. A simple probabilistic model aiming at the determination of bending resistance and vertical deflection of a simply supported prestressed concrete T-beam is built. Time dependent behavior of basic properties of concrete such as modulus of elasticity and compressive strength are approximated by suitable curves through data obtained from experiment. Monte Carlo simulation technique is used to take into account of the variation of input parameters. Normal distributions are assumed for random variability of elastic modulus and compressive strength of concrete as well as the change in position of tendons in the beam section. Relaxation loss of tendons is also considered. All procedures for analysis and simulation are composed using Matlab/Octave compatible environment. Bending moment resistance and vertical deflection of the beam are comparatively analyzed via numerical examples. Section of the prestressed concrete T-beam is then optimized with respect to its dimensions.

Keywords: beam, bending resistance, deflection, Monte Carlo simulation, prestressed concrete, probabilistic model, random, T-section, variation.

5.1. Introduction

Due to its conveniences in comparison with reinforced concrete and other building materials, prestressed concrete has become a popular material in construction for ages. Concept of prestressed concrete structures arose from the need of a concentric or eccentric force imposed in the longitudinal direction of the structural element to prevent crack development at early stages of loading (Nawy, 2009). In addition, the current trend is the improvement of concrete performance and reduction of the cement usage through using progressive high performance materials (Aitcin, 1998, Konecny *et al.*, 2017, Ghosh *et al.*, 2017,

Cajka *et al.*, 2017, Keulenl *et al.*, 2017). The more application of prestressed concrete in construction take place, the more research and study of advanced design methods for this type of structure is expected.

The rapid development of design methods for prestressed concrete structures has taken place during past decades (Nawy, 2009) and the trend is now focusing on the evaluation of capacities of advanced non-linear modelling (Králik and Klabník, 2016, Sucharda *et al.*, 2017). Deterministic and probabilistic theories have been both integrated in current codes and design standards (EN 1992-1-1, 2004, Matthews *et al.*, 2016) even though the first one is usually referencing and following by many engineers. In fact, input parameters governing resistances of prestressed concrete elements often show high variation and fluctuation. As a result, probability-based design approaches (Marek *et al.*, 2003, Melchers, 1999, Stewart and Rosowsky, 1998) for reinforced concrete and prestressed concrete structures are increasingly used nowadays.

Resistance of prestressed concrete beams based on probabilistic method has been recently studied for various purposes. Such a work e.g. (Le *et al.*, 2018) has been carried out to serve for the designing the full scale samples for the laboratory experiments of a simply supported beam with rectangular section. Results from (Le *et al.*, 2018) confirmed experience and expectations that rectangular high performance concrete (HPC) prestressed shape is not effective with respect to concrete utilization. The T-section or I-section beams are more effective comparing to rectangular one and they should be employed to fully utilize the potential of HPC. The calculation of the flexural strength of concrete T-beams was also discussed in many issues of the PCI (Precast Concrete Institute) Journal (Seguirant *et al.*, 2005). The work in (Seguirant *et al.*, 2005) examined the fundamentals of T-beam behavior at nominal flexural strength via a strain compatibility approach using non-linear concrete compressive stress distributions.

In this chapter, the preparation of a simple probability-based model for the bending resistance computation of a simply supported prestressed concrete T-beam is presented. The goal of this development is to prepare numerical codes for evaluation of bending resistance and deflection of the T-beam with respect to section optimization. Available time dependent behavior of basic properties such as compressive strength and elastic modulus of concrete is exploited. Scatter of input parameters is taken into account by using Monte Carlo simulation technique (Anderson, 1999). Random variability of elastic modulus and compressive strength of concrete as well as the change of position of tendons in the beam section is set up with the assumption of normal distributions. The approximation of relaxation loss of tendons is considered. Matlab/Octave compatible environment (www.mathworks.com,

www.octave.org) is adopted to compose procedures for facilitating all the simulations in this research.

5.2. Material properties

Time dependent modulus of elasticity and compressive strength are substantial properties governing behavior of prestressed concrete beams. The magnitudes of two properties may be approximated using Eurocode 2 (EN 1992-1-1, 2004), as follows:

$$E_{cm}(t) = (f_{cm}(t)/f_{cm})^{0.3} E_{cm} \quad (5.1)$$

and

$$f_{cm}(t) = \beta_{cc}(t) \cdot f_{cm} \quad (5.2)$$

where:

- $E_{cm}(t)$ – average modulus of elasticity (GPa) of concrete at age t (days)
- $f_{cm}(t)$ – average strength (MPa) of concrete in compression at age t (days)
- E_{cm} – mean modulus of elasticity (GPa) of concrete at 28 days
- f_{cm} – mean compressive strength at 28 days
- $\beta_{cc}(t)$ – coefficient depends on the age of the concrete

In this study, however, modulus of elasticity and compressive strength are approximated by suitable curves through data obtained from aging process of concrete sample with strength class of C50/60 from precast concrete production facility. Fig. 5.1 depicts the approximation of elastic modulus of such a sample case on which the magnitude of modulus of elasticity is approximated in a time by regression function, eq. 5.3.

$$E_{c,cyl}(t) = 4.3067 \ln(t) + 23.537 \quad (5.3)$$

where:

- $E_{c,cyl}(t)$ – elastic modulus (GPa) of a reinforced concrete tested sample at age t (days).

Similarly, approximation of the cylinder compressive strength is carried out based on the same laboratory sample. In this case, content from (Le *et al.*, 2018) is adopted, as shown in Fig. 5.2 and eq. 5.4.

$$f_{c,cyl}(t) = 12.845 \ln(t) + 33.627 \quad (5.4)$$

where:

- $f_{c,cyl}(t)$ – cylindrical strength (MPa) of a reinforced concrete tested sample at age t (days)

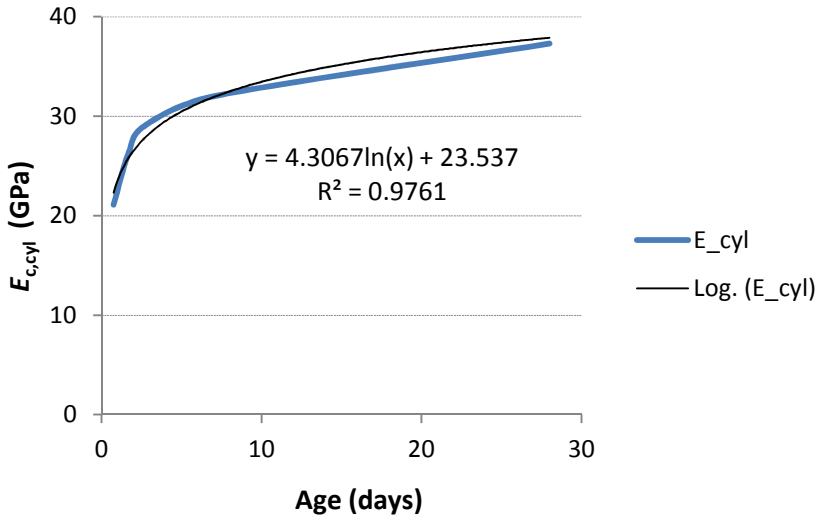


Fig. 5.1. Approximation of considered elastic modulus time dependent behavior

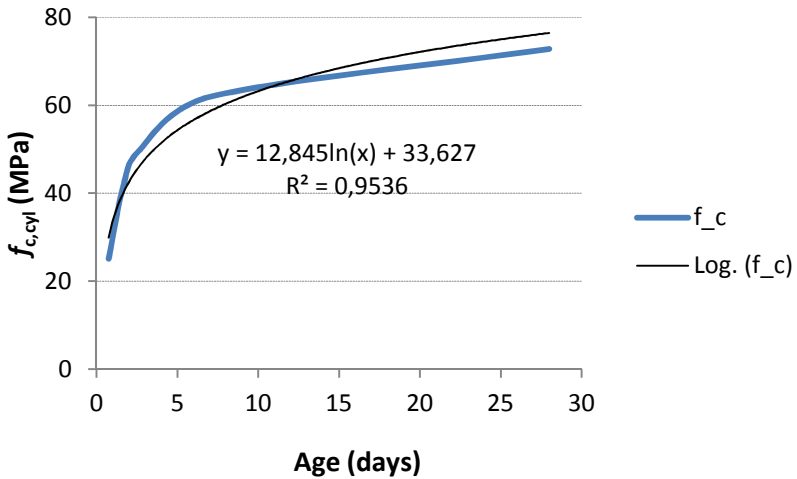


Fig. 5.2. Approximation of considered cylinder strength time dependent behavior (Le *et al.*, 2018)

It can be observed from Fig. 5.1 and Fig. 5.2 that the coefficients of determination in both cases are very good, $R^2 = 0.9761$ and $R^2 = 0.9536$, respectively. Therefore, the approximation in eq. 5.3 and eq. 5.4 has good fit.

As above mentioned that a simple probabilistic model is aimed at in this study, the statistic characteristics of probability density functions shall be studied and the variation of elastic modulus is described as follows:

$$E_{c,cyl}(t) = \mu(E_{c,cyl}(t)) + cov(E_{c,cube}(28)) \cdot \mu(E_{c,cyl}(t)) \quad (5.5)$$

where:

$E_{c,cyl}(t)$	–	elastic modulus (GPa) of sample at age t (days)
$\mu(E_{c,cyl}(t))$	–	mean value of elastic modulus of sample at age t
$cov(E_{c,cube}(28))$	–	coefficient of variation of elastic modulus of sample, $t = 28$ days

And then variation of concrete strength is:

$$f_{c,cyl}(t) = \mu(f_{c,cyl}(t)) + cov(f_{c,cube}(28)) \cdot \mu(f_{c,cyl}(t)) \quad (5.6)$$

where:

$f_{c,cyl}(t)$	–	cylindrical strength (MPa) of sample at age t (days)
$\mu(f_{c,cyl}(t))$	–	mean value of cylindrical strength of sample at age t
$cov(f_{c,cube}(28))$	–	coefficient of variation of cubic strength of sample, $t = 28$ days

5.3. Probabilistic modelling of T-beam resistance

5.3.1. Computational model for T-beam.

Without taking into account of reinforcement, ultimate bending moment resistance (M_r) of a critical T-section and prestressing tendons of a beam is computed according to 2 cases as follows:

* Case 1: Height of compression zone is larger than the flange thickness (Fig. 5.3):

$$M_r = F_{c1}(d - 0.4x) + F_{c2}(d - 0.5h_f), \quad (5.7)$$

where:

F_{c1} – compressive forces (kN) in concrete due to the contribution of web,

F_{c2} – compressive forces (kN) in concrete due to the contribution of flange.

They are determined as:

$$F_{c1} = 0.8f_{c,cyl}b_w x, \quad (5.8)$$

$$F_{c2} = 0.8f_{c,cyl}(b - b_w)h_f, \quad (5.9)$$

where:

d	–	effective height (m) of considering cross section of the beam
x	–	height of compression zone (m), calculated based on the limit strain approach (strain compatibility), as follows:

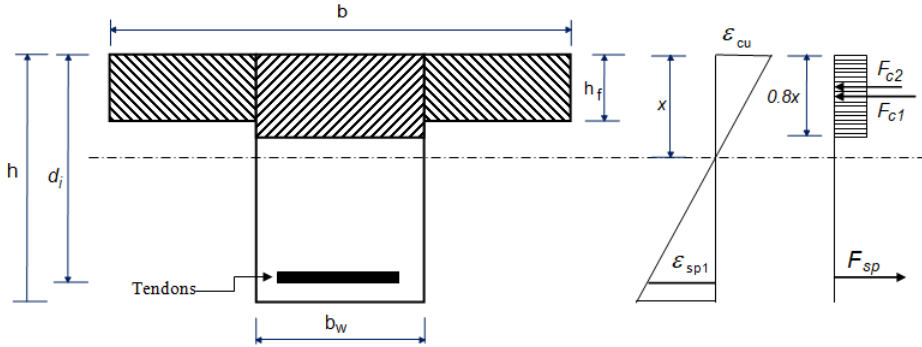


Fig. 5.3. Sketch of a cross-sectional T-beam in the computation model

$$x = \frac{F_{sp} - F_{c2}}{0.8f_{c,cyl}b_w} \quad (5.10)$$

- b_w – thickness (m) of the web of T-beam
 b – width (m) of the flange of T-beam
 h_f – thickness (m) of flange of T-beam,
 $f_{c,cyl}$ – cylinder compressive strength (kPa) of concrete
 F_{sp} – total prestressing force (kN) in all layers of tendons after relaxation losses, computed as:

$$F_{sp} = \sum N_{xi} A_p \sigma_{pst}, \quad (5.11)$$

where:

- N_{xi} – number of tendons horizontally in layer i
 A_p – cross-sectional area (m²) of prestressing tendon
 σ_{pst} – prestressing stress (kPa) after relaxation losses, determined as:
- $$\sigma_{pst} = \sigma_{pmax} \text{ if } t < 72 \text{ hours} \quad (5.12a)$$
- $$\sigma_{pst} = \sigma_{pmax} \times 0.85 \text{ if } 72 \text{ hours} \leq t < 500,000 \text{ hours,} \quad (5.12b)$$
- $$\sigma_{pst} = \sigma_{pmax} \times 0.85 \times 0.85 \text{ if } t \geq 500,000 \text{ hours,} \quad (5.12c)$$

where:

- σ_{pmax} – maximum prestressing stress (kPa) of tendons.

* Case 2: Height of compression zone is smaller than the flange thickness (behaves as rectangular section):

$$M_r = F_c(d - 0.4x), \quad (5.13)$$

where:

F_c – compressive forces (kN) in concrete, calculated as:

$$F_c = 0.8f_{c,cyl}bx \quad (5.14)$$

x – height of compression zone (m), calculated as:

$$x = \frac{F_{sp}}{0.8f_{c,cyl}b} \quad (5.15)$$

Instant deflection at middle of this simply supported beam in the time when the test of ultimate carrying capacity is conducted:

$$w = w_g + w_p + w_F, \quad (5.16)$$

where:

w – total deflection (m) at the middle of the beam

w_g – deflection (m) at the middle of the beam due to dead load:

$$w_g = \frac{5}{384}g \frac{l^4}{EI} \quad (5.17)$$

g – dead load (kN/m) due to self weight of the beam,

$$g = 9.81 \times A \times \rho / 1000 \quad (5.18)$$

A – cross-sectional area of T-beam

ρ – unit weight (kg/m³) of concrete

E – elastic modulus (kPa) of concrete

I – inertia moment (m⁴) of T-section

L – loading span (m) of the beam

w_p – deflection (m) at the middle of the beam due to prestressing force:

$$w_p = \frac{1}{8}M_p \frac{l^2}{EI}, \quad (5.19)$$

M_p – bending moment (kNm) due to eccentricity of prestressing forces:

$$M_p = -F_{sp}e, \quad (5.20)$$

E – eccentricity (m) of prestressing forces

w_F – deflection (m) at the middle of the beam due to induced moment without prestressing:

$$w_F = \frac{1}{48}F \frac{l^3}{EI}, \quad (5.21)$$

F – ultimate force for bending of the T-beam:

$$F = \frac{4M_r}{l} \quad (5.22)$$

M_r – ultimate bending moment resistance (kNm) given in eq. 5.7 or eq. 5.13.

5.3.2. Monte Carlo simulation technique.

Monte Carlo approach is one of the popular simulation techniques allowing obtaining numerical results through a process of repeated random sampling. It uses random sampling and statistical modelling to estimate mathematical functions and mimic the operations of complex systems (Harrison, 2010). It can be considered as the art of approximating an expectation by the sample mean of a function of simulated random variables (Anderson, 1999). It was used in (Le *et al.*, 2018) to consider time dependent variation of carrying capacity of prestressed rectangular beam. Creating the sample, running the model and analyzing the data are the three main steps of this method.

5.3.3. Transformation and generation of random variables.

A desired distribution of a parameter can be modeled using the following formula (Fegan and Gustar, 2003):

$$N(\mu, \sigma) = \mu + \sigma \times N(0,1), \quad (5.23)$$

where:

- μ – specified mean value
- σ – specified standard deviation
- $N(0,1)$ – represents random numbers from the normalized normal distribution
- $N(\mu, \sigma)$ – represents random numbers from the generated normal distribution

For time dependent parameters, their distribution can be written as:

$$N(\mu, \sigma, t) = \mu(t) + \sigma(t) \times N(0,1), \quad (5.24)$$

where:

- $N(\mu, \sigma, t)$ – represents time dependent normal distribution from the normalized one at age t ,
- $\mu(t)$ – specified time dependent mean value at age t (days)
- $\sigma(t)$ – specified time dependent standard deviation at age t

In addition, desired uniform distribution of a parameter can also be modeled using available commands in Matlab/Octave.

5.4. Numerical examples

For illustrative purpose, examples of calculation of resistance and vertical deflection of a prestressed concrete T-beam is presented in this part. Bending resistance and deflection of the beam will also be analyzed with respect to section optimization.

It is a simply supported prestressed concrete T-beam with dimensions of cross section as depicted in Fig. 5.4.

In order to compare results of this analysis with those of (Le *et al.*, 2018), a width of 0.9 m is assigned for the flange and the height of 0.56 m of the beam is selected. The length of the beam is 7 m. There are 3 layers of bottom tendons with 4 wires each. Area of one-wire prestressing tendon is $A_p = 150 \times 10^{-6} \text{ m}^2$. Distance between the two layers of tendons is 0.05 m and a 0.08 m concrete cover is assumed. Effect of conventional reinforcement is neglected in this study. Its effect in case of ultimate carrying capacity is limited comparing to prestressing tendons. The cross-sectional bending resistance of the beam will be investigated by implementation of the above set up model in combination with Monte Carlo simulation technique.

To verify the prepared procedure, however, this example is solved by both deterministic and probabilistic methods.

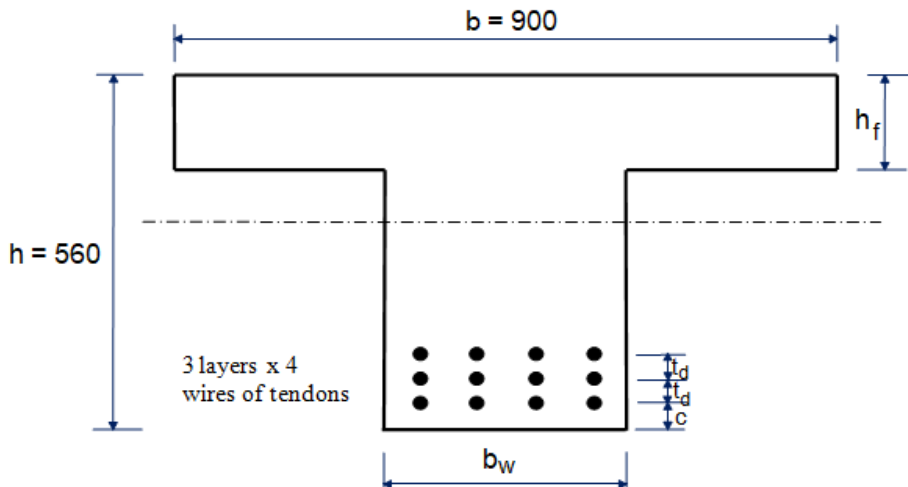


Fig. 5.4. Cross section of considered T-beam

5.4.1. Deterministic solution.

Input parameters for deterministic problem are as follows:

- Geometry: $h = 0.56 \text{ m}$, $b = 0.9 \text{ m}$, $h_f = 0.18 \text{ m}$, $b_w = 0.31 \text{ m}$, $c = 0.08 \text{ m}$, $t_d = 0.05 \text{ m}$, $d = 0.52 \text{ m}$, $l = 7 \text{ m}$.

→ Cross-sectional area $A = 0.2798 \text{ m}^2$ and inertia moment: $I = 0.0072 \text{ m}^4$.

- Concrete properties:

- + Unit weight: $\rho = 2390 \text{ kg/m}^3$,
- + Elastic modulus: $E_c = 26.522 \text{ kPa}$,

- + Compressive strength: $f_{c,cyl} = 42.531$ kPa.
- Prestressing tendons:
 - + Cross-sectional area of one wire of tendon: $A_p = 150 \times 10^{-6}$ m²,
 - + 0.1% proof-stress of prestressing steel: $f_{p01} = 1687 \times 10^3$ kPa,
 - + Maximum prestressing stress of tendon: $\sigma_{pmax} = 1400 \times 10^3$ kPa.
- Limit strain of concrete and steel:
 - + Maximum strain at the compression fiber of concrete at strength limit state (BS 8110-1, 1997 and EN 1992-1-1, 2004): $\epsilon_{cu} = 0.0035$,
 - + Limit deformation in steel of prestressed reinforced concrete elements at ULS (EN 1994-1-1, 2004): $\epsilon_{ud} = 0.02$.

Results of the problem with deterministic computation are summarized in Table 5.1. The deflections represent values related to the time of the carrying capacity with the load imposed in the day of testing.

It is important to note that the cross-sectional area (A) of T-beam used in the computation is only 0.2798 m², about 55.52 % of cross-sectional of rectangular beam (0.504 m²) studied in (Le *et al.*, 2018).

Table 5.1. Results from deterministic analysis of considered T-beam ($A = 0.2798$ m²)

Deterministic analysis results with $A = 0.2798$ m ²	$t < 3$ days = 72 hours (at $t = 2$ days)	72 hours $\leq t < 500.000$ hours (at $t = 14$ days)	$t \geq 500.000$ hours (at $t = 28$ days)
Bending moment resistance, M_r (kNm)	1,227.4	1,076.1	1,080.5
Vertical deflection, w , at middle of the beam under the ultimate loading (m)	0.0200	0.0135	0.0125

In order to observe the effectiveness of prestressed concrete section type under bending, another cross-sectional T-beam with area of 0.5018 m² ($h = 1.2$ m, $h_f = 0.22$ m, $d = 1.12$ m, other dimensions are keep unchanged) is analyzed, i. e. cross-sectional area of T-beam in this study and that of rectangular one in (Le *et al.*, 2018) are almost the same. The results are shown in Table 5.2.

Table 5.2. Results from deterministic analysis of considered T-beam ($A = 0.5018 \text{ m}^2$)

Deterministic analysis results with $A = 0.5018 \text{ m}^2$	$t < 3$ days = 72 hours (at $t = 2$ days)	72 hours $\leq t < 500.000$ hours (at $t = 14$ days)	$t \geq 500.000$ hours (at $t = 28$ days)
Bending moment resistance, M_r (kNm)	2,739.4	2,361.3	2,365.7
Vertical deflection, w , at middle of the beam under the ultimate loading (m)	0.0047	0.0031	0.0029

Here, we make a comparison of bending moment resistance between T-section in this research and rectangular section in (Le *et al.*, 2018).

Since results of work in (Le *et al.*, 2018) are probabilistic, only mean values of those results will be used to compare as described in Table 5.3. In addition, case of $t = 14$ days was not studied in (Le *et al.*, 2018). Therefore, case $t = 2$ days and $t = 28$ days are compared.

Table 5.3. Bending resistance of considered T-section in this study versus bending resistance of rectangular section investigated in (Le *et al.*, 2018)

Age of concrete (days)	Bending moment resistance, M_r (kNm)			Increase (+) / Decrease (-) of M_r	
	T-section, $A = 0.2798\text{m}^2$ (a)	T-section, $A = 0.5018\text{m}^2$ (b)	Rectangular section, $A = 0.504\text{m}^2$ (Le <i>et al.</i> , 2018) (c)	(a) vs. (c)	(b) vs. (c)
$t = 2$	1,227.4	2,739.4	1,458.4	- 15.8 %	+ 87.8 %
$t = 28$	1,080.5	2,365.7	1,511.8	- 28.5%	+ 56.5%

It is worth noticing from Table 5.3 that at almost the same cross-sectional area (b and c), bending resistance of the beam can be increased to 87.8 % (at $t = 2$ days) and 56.5 % (at $t = 28$ days) if T-section is used instead of rectangular one. It is important to mention that in case of rectangular section (Le *et al.*, 2018), the relaxation losses were not considered. Thus the bending resistance increases due to the increase of concrete strength over the time. Furthermore, even though the cross-sectional area is reduced 44.48 % in comparison with rectangular section, the bending moment resistance of the T-beam decreases only 15.8 % and 28.5 % at $t = 2$ days and $t = 28$ days, respectively. It is likely that the

reduction in bending resistance of T-beam in this study is partly caused by relaxation losses (15 % since 3 days and 22.5 % after 500,000 hours). Therefore, it is confirmed that T-section is a better choice than rectangular section for prestressed precast concrete beam with respect to bending. Resulted maximum deflection at the middle of the beam under ultimate loading via deterministic method is 0.020 m, equals to allowable deflection of the beam, $w_{lim} = 1/350$ of beam span = 7 m/350 = 0.020 m (ACI 318-08, 2008).

5.4.2. Probabilistic solution.

Table 5.4. Information on input parameters employed in the probabilistic study

Parameter	Notation	Mean	Coefficient of variation	Transformation
Elastic modulus of concrete (kPa)	$E_{c,cyl}(t)$	eq. 5.1	0.0388	$\mu(E_{c,cyl}(t)) + 0.0388 \times N(0,1)$
Concrete strength (kPa)	$f_{c,cyl}(t)$	eq. 5.2	0.0388	$\mu(f_{c,cyl}(t)) + 0.0388 \times N(0,1)^{(*)}$
Effective height of the beam (m)	d	0.52	0.0096	$d = 0.52 + 0.005 \times N(0,1)$
Thickness of the web (m)	b_w	0.31	-	-
Thickness of the flange (m)	h_f	0.18	-	-
Loading span (m)	l	6.85	-	-
Width of flange of the considered beam (m)	b	0.9	-	-
Height of cross section of the beam (m)	h	0.56	-	-
Cross-sectional area of prestressing tendons (m ²)	A_p	150×10^{-6}	-	-
0.1% proof-stress of prestressing steel (kPa)	f_{p01}	1687×10^3	-	-
Thickness of concrete covered layer (m)	c	0.08	-	-

(*): Please be noted that $E_{c,cyl}(t)$ and $f_{c,cyl}(t)$ are considered as uncorrelated parameters here.

Input parameters for probability-based analysis are presented in Table 5.4. Eq. 5.23 is used to build up histograms of elastic modulus, cylinder compressive strength of concrete and effective height of considered cross section of the T-beam. Ultimate bending moment resistance of the critical T-section is computed by eq. 5.7 or eq. 5.13.

In this study, effect of conventional reinforcement is neglected as mentioned above. So, the resistance is provided by concrete and prestressed tendons. Fig.

5.5 displays the distribution of bending moment resistance of the cross section of the T-beam at different ages of concrete.

It is remarkable from the figure that bending moment resistance of the cross section at different ages of concrete follow normal distributions and these distributions are not the same with concrete aging. This result is quite similar to that of (Le *et al.*, 2018).

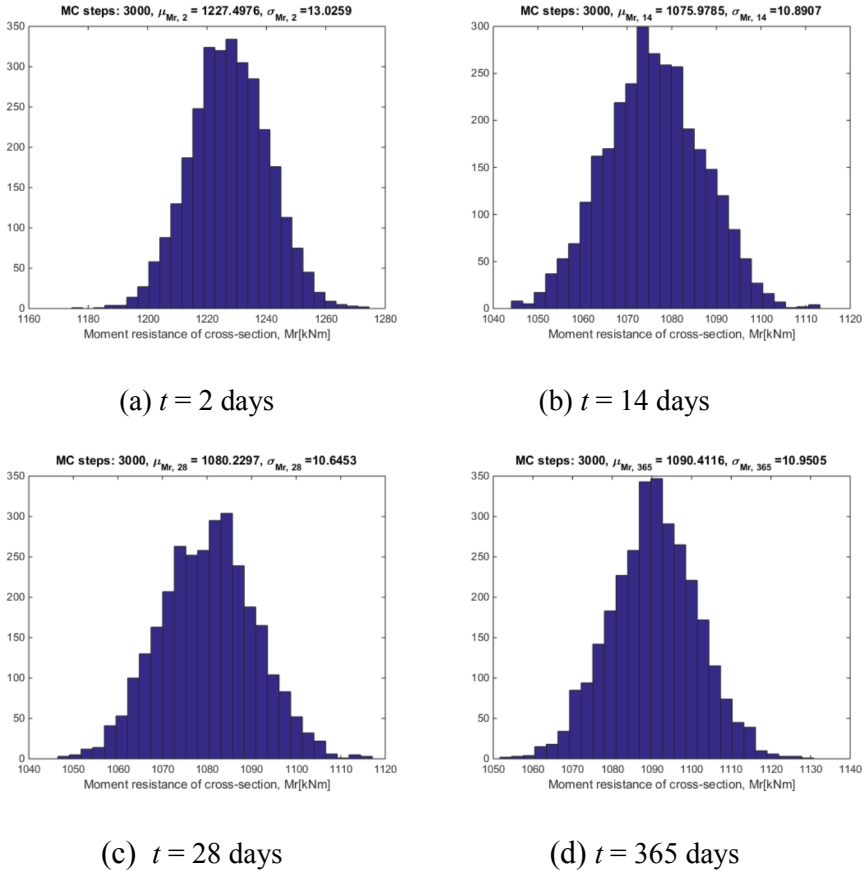
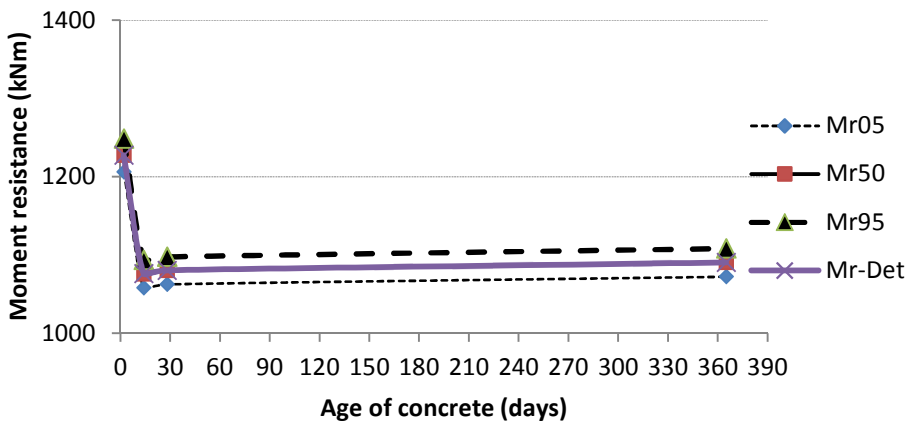


Fig. 5.5. Distribution of bending moment resistance of the cross section of the T-beam

Simulation results on bending moment resistance of cross section of the T-beam and their confidence bounds are summarized in Table 5.5 and illustrated in Fig. 5.6 together with results from deterministic solution, marked as M_r -Det in the figure.

Table 5.5. Simulation results on bending moment resistance of cross section of the T-beam

Age of concrete t (days)	Bending moment resistance of the cross section of the T-beam (kNm)			
	M_{r05} (5%)	M_{r50} (50%)	M_{r95} (95%)	Deterministic analysis
2	1,206.072	1,227.498	1,248.923	1,227.4
14	1,058.065	1,075.979	1,093.892	1,076.1
28	1,062.720	1,080.230	1,097.740	1,080.5
365	1,072.400	1,090.412	1,108.424	1,090.5

**Fig. 5.6.** Bending moment resistance of the cross section of the T-beam

It can be seen from Table 5.5 and Fig. 5.6 that values of bending resistance from deterministic calculation are almost the same with mean values resulted from probabilistic simulations. This means that the built up probabilistic model works well.

Fig. 5.6 also displays that moment resistance of the T-section sharply decreases in the first two weeks before gradually increasing from the 3rd week onwards. The drop trend in this duration is inversed in compare with that of (Le *et al.*, 2018). This can be explained by the fact that relaxation losses were not taken into account in (Le *et al.*, 2018). In addition, it can be observed from Fig. 5.6 that the variation of bending resistance is insignificant, around of ± 2 percent.

In the mean time, results on vertical deflection (w_{prob}) at middle of the beam are shown in Table 5.6 and Fig. 5.7 together with those of deterministic computation and maximum allowable vertical deflection specified by design code (w_{lim}).

Table 5.6. Results on vertical deflection of the T-beam

Age of concrete t (days)	Vertical deflection (m) at the middle of the T-beam	
	Probabilistic solution (maximum value)	Deterministic solution
2	0.0166	0.0200
14	0.0111	0.0135
28	0.0113	0.0125
365	0.0092	0.0098

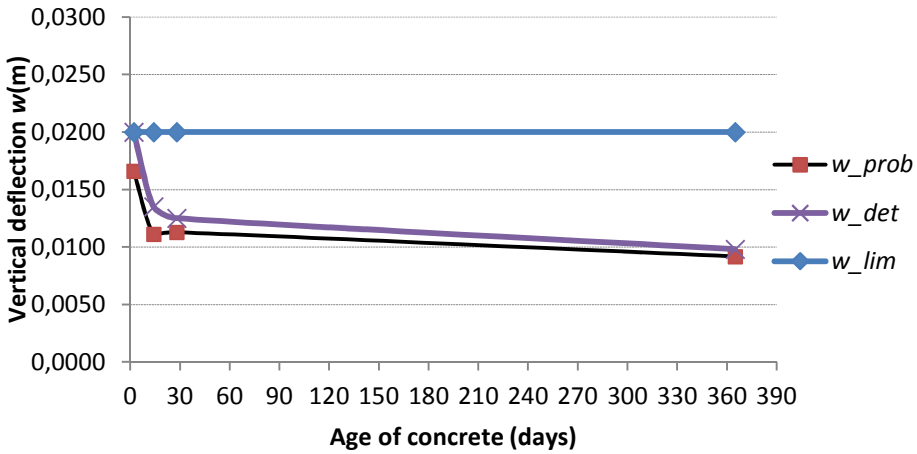


Fig. 5.7. Vertical deflection at middle of the T-beam

It can be observed from Table 5.6 and Fig. 5.7 that deterministic calculation produces higher values of deflection than probabilistic analysis does. It needs to be underlined also that the differences in values of deflection resulted from between the two methods are small and these are almost negligible. Fig. 5.7 also showed that vertical deflection of considered T-beam is still in allowable limit because the two curves w_{prob} and w_{det} locate beneath the curve w_{lim} .

5.4.3. Section optimization.

Through above deterministic computation and probabilistic simulations of considering T-beam, the set up probability-based model has been verified. It can be developed more in order to apply for section optimization.

Continuing this numerical example, resistance of the cross section will be investigated on the basis of variation of flange thickness (h_f) and web thickness (b_w). Uniform distribution of these two parameters is given in range for the

optimization. However, to have practical dimensions of cross section of the T-beam, minor revision of these two parameters' range of variation was made to generate values from the uniform distribution on the reasonable intervals. Thickness of the web is allowed to vary from 0.286 m to 0.610 m to meet requirement of minimum clear spacing between pre-tensioned tendons (EN 1992-1-1, 2004) while thickness of the flange fluctuates from 0.14 m to 0.36 m. Width of the flange and height of the beam are kept unchanged. Partial results on section optimization are summarized in Tables 5.7, 5.8 and 5.9.

Table 5.7. Partial simulation results on section optimization of considered T-beam at $t = 2$ days

Age of concrete, t (days)	Maximum resistance, $max_Mr = 1271.0$ kNm		Minimum vertical deflection, $min_w = 1.095 \times 10^{-7}$ m		Maximum vertical deflection, $max_w = 0.127$ m	
	b_w (m)	h_f (m)	b_w (m)	h_f (m)	b_w (m)	h_f (m)
2	0.408	0.242	0.406	0.257	0.334	0.243

Table 5.8. Partial simulation results on section optimization of considered T-beam at $t = 14$ days

Age of concrete, t (days)	Maximum resistance, $max_Mr = 1113.1$ kNm		Minimum vertical deflection, $min_w = 6.653 \times 10^{-8}$ m		Maximum vertical deflection, $max_w = 0.096$ m	
	b_w (m)	h_f (m)	b_w (m)	h_f (m)	b_w (m)	h_f (m)
14	0.582	0.228	0.561	0.164	0.452	0.296

Table 5.9. Partial simulation results on section optimization of considered T-beam at $t = 28$ days

Age of concrete, t (days)	Maximum resistance, $max_Mr = 1122.3$ kNm		Minimum vertical deflection, $min_w = 6.641 \times 10^{-8}$ m		Maximum vertical deflection, $max_w = 0.080$ m	
	b_w (m)	h_f (m)	b_w (m)	h_f (m)	b_w (m)	h_f (m)
28	0.396	0.220	0.501	0.358	0.415	0.326

In order to observe how the geometry of the T-section is at maximum bending resistance, their visual relations could be captured in figures. For instance, Fig. 5.8 describes relation between geometry of the section and its bending moment resistance in case of time $t = 28$ days.

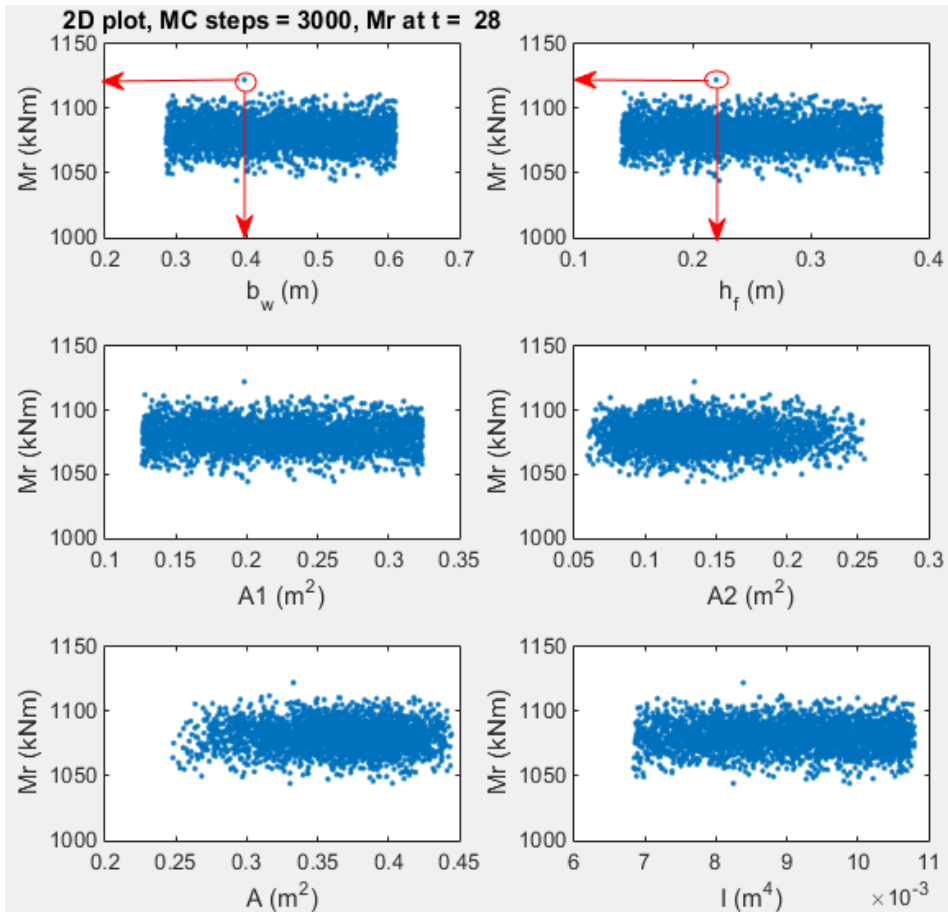


Fig. 5.8. Relations between bending resistance and geometry of the T-section at $t = 28$ days

From Fig. 5.8, it is possible to find out web thickness and flange thickness in accordance with maximum bending resistance of the T-section at specific age of concrete of 28 days. Red ellipses and arrows on this figure illustrate the way to pick up specific dimensions of optimal section with respect to maximum bending resistance of the T-beam. Other parameters of section such as area of the flange (A_1), area of the web (A_2), total cross sectional area (A) and inertia moment (I) when bending resistance reaches maximum value can also be picked up in the same way. Similarly, relations between vertical deflections and geometry of the T-section can be intuitively depicted in figures. Fig. 5.9, for example, displays the relation between geometry of the section and its vertical deflections in case of time $t = 28$ days.

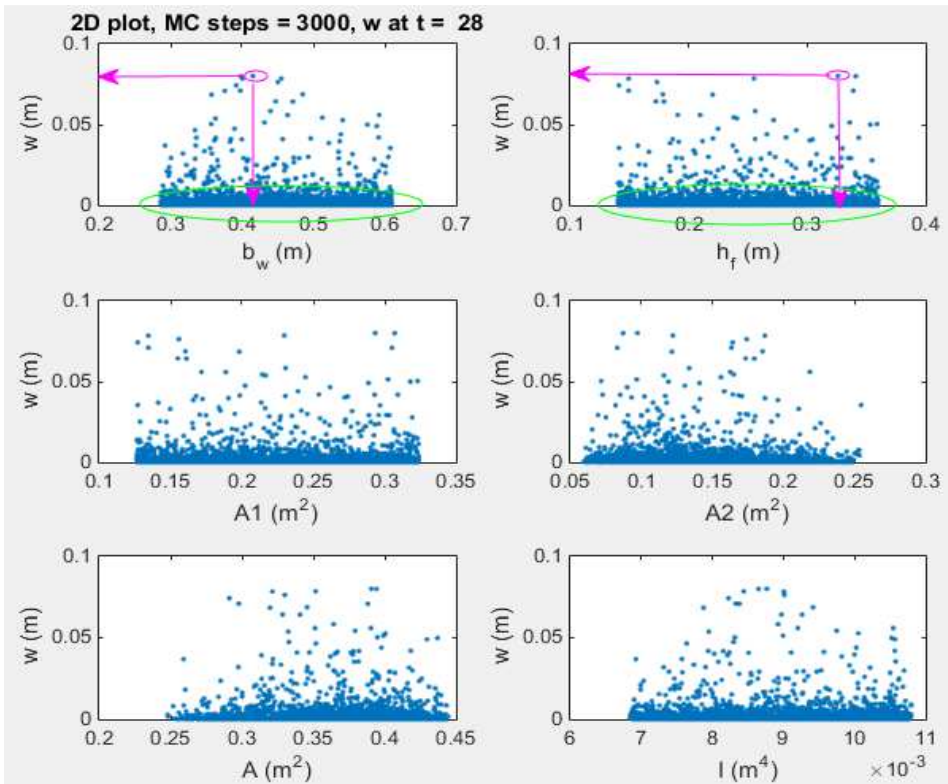


Fig. 5.9. Relations between vertical deflections and geometry of the T-section at $t = 28$ days

In the case of maximum vertical deflection is targeted, intuitive observation of accordingly geometry dimensions of the section is quite easy based on Fig. 5.9 (marked pink ellipses and arrows).

However, if minimum of vertical deflection of the T-section is aimed, visual identification of accordingly geometry dimensions becomes difficult. As marked by large green ellipses in Fig. 5.9, there are a wide range of web thickness and flange thickness values at very low vertical deflections. In these situations, picking up specific values of these dimensions should be done directly with results in numerals from the built up code as summarized in above Tables 5.7, 5.8 and 5.9. Identification of other geometry parameters of the T-section could also be carried out in the same ways.

Meanwhile, general interaction between bending resistances of the T-section and its vertical deflections are displayed in Fig. 5.10 in case of time $t = 28$ days, as illustrative purpose.

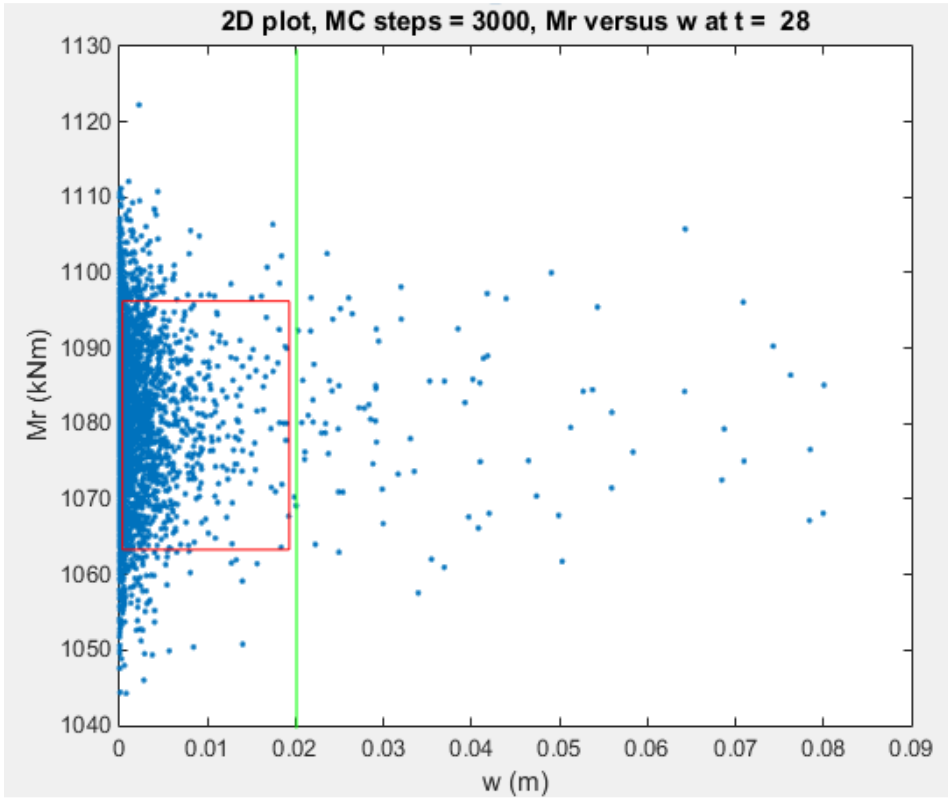


Fig. 5.10. Interaction between resistance and vertical deflections of the T-section at $t = 28$ days

It is remarkable from Fig. 5.10 that the bending resistance of considering T-section has normal distribution. This is consistent with results described in Fig. 5.5. In the relationship with vertical deflection of the section, the zone of mean value spectrum of bending resistance (marked by red rectangle in Fig. 5.10) locates on the left hand side of the limit line of allowable maximum vertical deflection in this example (marked as green line).

To obtain overall results of section optimization, another procedure is composed with 2 conditions: (i) vertical deflection (w) of the cross section is always smaller than maximum allowable vertical deflection (w_{lim}); (ii) bending moment resistance of the cross-sectional T-beam (M_r) is larger than minimum value of bending moment resistance of the beam at concrete age of 28 days.

Table 5.10. Overall simulation results on section optimization of considered T-beam at $t = 28$ days (10 options of best scores)

Option No.	Vertical deflection			Bending resistance			Area of cross section			Score (%)
	w (m)	Percentage of the best (%)	weight	M_r (kNm)	Percentage of the best (%)	weight	A (m ²)	Percentage of the best (%)	weight	
1	7.6×10^{-6}	93	0.3	1098.8	95	0.2	0.2743	97	0.5	95.4
2	1.3×10^{-6}	97	0.3	1100.9	96	0.2	0.2897	94	0.5	95.3
3	1.2×10^{-7}	99	0.3	1101.5	97	0.2	0.3016	90	0.5	94.1
4	7.8×10^{-7}	98	0.3	1095.3	90	0.2	0.2940	93	0.5	93.9
5	2.9×10^{-6}	96	0.3	1090.6	81	0.2	0.2877	95	0.5	92.5
6	8.1×10^{-6}	93	0.3	1086.9	71	0.2	0.2593	99	0.5	91.6
7	8.6×10^{-6}	93	0.3	1092.6	85	0.2	0.2933	93	0.5	91.4
8	6.4×10^{-5}	81	0.3	1092.8	86	0.2	0.2532	99	0.5	91.0
9	6.3×10^{-5}	81	0.3	1100.1	96	0.2	0.2810	95	0.5	91.0
10	1.1×10^{-6}	97	0.3	1098.4	94	0.2	0.3110	86	0.5	90.9

However, the considered problem has many parameters changing with geometry such as deflection and resistance. In addition, results of optimization process strongly depend on its target. Therefore, determination of target for the optimization problem is significantly important. In this example, weight function has been used to make decision of optimal geometry. An example of results presented in Table 5.10 on which weights of deflection, bending moment resistance and cross-sectional area of the T-beam are 30%, 20% and 50%, respectively. The weight factor of 50% reveals that reducing volume of concrete is aimed at in this study.

Table 5.10 is considered as a tool to suggest the best option for section optimization of the T-beam based on the best overall score with specified weight function. Only 10 best options (descendent order) were shown for

illustrative purpose. In case of option number 1 (the best score among 10 options in Table 5.10) is selected, for instance, the corresponding dimensions of T-beam are $b_w = 0.3079$ m, $h_f = 0.1721$ m.

If weight function is changed to meet new targets of optimal problem, values in the last column of Table 5.10 would be changed and hence new decision would be made.

5.5. Conclusions

The model used for the analysis of behavior of prestressed precast beam may be used for preliminary analysis of bending resistance with respect to preparation of full scale testing at laboratory conditions. Also important part is shape parameters' optimization capability via application of simple Monte Carlo based technique and weight function.

Computation of bending resistance and vertical deflection over the time of a prestressed precast concrete T-beam was done through a new built simple probabilistic model. Randomness of input parameters such as elastic modulus and compressive strength of concrete as well as position of tendons in the section was taken into account with assumption of normal distributions. The performance of the T-beam under prestressing was studied via numerical examples by application of Monte Carlo simulation technique. Dimensions of T-section of the beam in the example were also optimized targeted at minimum cross-sectional area, maximum bending resistance and best performance of vertical deflections.

As expected, results of the study confirmed that T-section is a better choice in comparison with rectangular one for prestressed precast concrete beam in bending resistance. In this study, for example, with almost the same cross-sectional area, bending resistance of the T-beam was about 187.8 % (at $t = 2$ days) and 156.5 % (at $t = 28$ days) of that of the rectangular one.

Investigation of vertical deflection of the considered T-beam shown that under conditions in the example, vertical deflection of the beam is still in allowable limit. Therefore, selected dimensions of the section are suitable enough for performance of the beam in such a case.

Optimization results proved their consistence and coherence with those of bending resistance computation part. So, the built procedure for section optimization seems to be applicable for prestressed precast concrete T-beam.

The current study deals only with prestressing tendons from bottom part of the section. In addition, influences of conventional reinforcement to performance of the T-beam were not considered. Furthermore, shear resistance and cracking

were not also been studied yet. This work, therefore, should be further developed with taking into account of tendons in the top part of the section and longitudinal reinforcement. Impacts of shear resistance and cracking would be expected expansion of the topic.

References

- ACI 318-08 (2008) 'Building Code Requirements for Structural Concrete and Commentary', *American Concrete Institute*, 38800 Country Club Drive Farmington Hills, MI 48331, ISBN 978-0-87031-264-9.
- Aitcin, P. C. (1998) 'High performance concrete', *Taylor & Francis*, ISBN-10: 0419192700, ISBN-13: 978-0419192701.
- Anderson, E. C. (1999) 'Monte Carlo methods and importance sampling - Lecture notes for Stat 578C', *Statistical Genetics*.
- BS 8110-1 (1997) 'Structural use of concrete. Code of practice for design and construction', *British Standards Institution*, ISBN 978 0 580 59893 7.
- Cajka, R., *et al.* (2017) 'Stress and strain of fiber reinforced concrete composites', *Proc. 6th Int. Conf. Non-traditional Cement & Concrete*, June 19-22-2017, Brno.
- EN 1992-1-1 (2004) 'Eurocode 2: Design of concrete structures - Part 1-1: General rules and rules for buildings', *The European Union Per Regulation 305/2011*.
- EN 1994-1-1 (2004) 'Eurocode 4: Design of composite steel and concrete structures – Part 1-1: General rules and rules for buildings', *The European Union Per Regulation 305/2011*.
- Fegan, G. and Gustar, M. (2003) 'Chapter 2 – Monte Carlo Simulation' in: Marek, P. *et al.* (2003) 'Probabilistic Assessment of Structures using Monte Carlo Simulation - Background, Exercises and Software', TeReCo 2nd edition, *Institute of Theoretical and Applied Mechanics*, Academy of Sciences of Czech Republic, Praha.
- Ghosh, P. *et al.* (2017) 'Probabilistic time-dependent sensitivity analysis of HPC bridge deck exposed to chlorides', *J. Computers and Concrete*, 19(3), pp. 305-313. DOI: <https://doi.org/10.12989/cac.2017.19.3.305>.
- GNU Octave Scientific programming language on-line: www.octave.org.
- Harrison, L. R. (2010) 'Introduction to Monte Carlo simulation', *AIP Conference Proceedings* 1204, 17(2010), doi: 10.1063/1.3295638.
- Keulenl, A. *et al.* (2017) 'Durability evaluation of aam using a plasticizing additive, enhancing fresh concrete rheology', *Proc. 6th Int. Conf. Non-traditional Cement & Concrete*, June 19-22-2017, Brno.
- Konecny, P. *et al.* (2017) 'Variation of diffusion coefficient for selected binary and ternary concrete mixtures considering concrete aging effect', *Proc. 6th*

- Int. Conf. Non-traditional Cement & Concrete*, June 19-22-2017, Brno.
- Králik, J. and Klabník, M. (2016) 'Nonlinear analysis of the failure of nuclear hermetic reinforced concrete structure due to extreme pressure and temperature', *Transactions of the VŠB – Technical University of Ostrava Civil Engineering Series*, 16(2), paper#17.
- Le, D. T. *et al.* (2018) 'Time dependent variation of carrying capacity of prestressed precast beam', *IOP Conference Series: Earth and Environmental Science*, 143(2018) 012013, IOP Publishing, doi:10.1088/1755-1315/143/1/012013.
- Marek, P. *et al.* (2003) 'Probabilistic Assessment of Structures using Monte Carlo Simulation - Background, Exercises and Software', TeReCo 2nd edition, *Institute of Theoretical and Applied Mechanics*, Academy of Sciences of Czech Republic.
- MatLab: The language of technical computing *MathWorks* - on-line: www.mathworks.com.
- Matthews, *et al.* (2016) 'Fib model code 2020 – A new development in structural codes: Towards a general code for both new and existing concrete structures', edited by Beushausen, H. (2016) 'Proc. fib Symp', *Performance-based approaches for concrete structures*, Cape Town, pp. 22-31.
- Melchers, R. (1999) 'Structural reliability analysis and prediction (Civil Engineering)', *Wiley*, West Sussex.
- Nawy, E. G. (2009) 'Prestressed concrete - a fundamental approach, 5th edition update', *Prentice Hall*, Upper Saddle River, New Jersey 07458, ISBN-10: 0-13-608150-9, ISBN-13: 978-0-13-608150-0.
- Seguirant, S. J. *et al.* (2005) 'Flexural strength of reinforced and prestressed concrete T-beams', *PCI Journal*, January-February 2005, pp. 44-73.
- Stewart, M. G. and Rosowsky, D. V. (1998) 'Time-dependent reliability of deteriorating reinforced concrete bridge decks', *Structural Safety*, 20(1), pp. 91-109.
- Sucharda, O. *et al.* (2017) *Periodica Polytechnica Civil Engineering*, 61(4), pp. 972-986.